Core-Penetrating Rydberg Series of BaF: $s \sim p \sim d \sim f$ Supercomplexes

Zygmunt J. Jakubek and Robert W. Field
Department of Chemistry, Massachusetts Institute of Technology, Cambridge, Massachusetts 02139

(Received 23 July 1993)

130 new vibronic Rydberg states of BaF are observed and assigned to 74 new electronic states. These states are arranged into 10 Rydberg series (four $^2\Sigma^+$, three $^2\Pi$, two $^2\Delta$, and one $^2\Phi$) spanning the region of effective principal quantum number $4.4 < n^*_{l\lambda} < 14.3$. All of the expected bound valence and core-penetrating Rydberg states of BaF belong to these ten series, which are the first examples of $s \sim p \sim d \sim f$ supercomplexes. The $n^*_{l\lambda}$ evolution of the quantum defects ($\mu_{l\lambda} \equiv n - n^*_{l\lambda}$) and fine structure constants (A, γ) are presented. The ionization potential is IP(BaF) $= 38\,742 \pm 3$ cm^{-1}.

PACS numbers: 35.20.My, 34.80.Kw, 35.20.Sd, 35.20.Vf

Even though Rydberg states of diatomic molecules have been studied for many years, little work has been done on systems with highly polar molecular-ion cores. Of all diatomic molecules, the alkaline earth monohalides seem to be the best examples of such systems. They have the simple (two closed shell atomic ions, M^{2+} and X^-) yet highly polar MX^+ molecular-ion core. Murphy *et al.* [1], Murphy [2], and Berg *et al.* [3] recorded and analyzed Rydberg spectra of CaF. They observed and characterized the *complete* manifold of core-penetrating Rydberg states (three $^2\Sigma^+$, two $^2\Pi$, and one $^2\Delta$ series) over the range of effective principal quantum number $4 < n^*_{l\lambda} < 10$. Their studies revealed substantial l mixing in all but the $d\delta$ series and the resultant formation of $s \sim p \sim d$ supercomplexes. This observation was confirmed by a quantum defect theory calculation of the Rydberg states of CaF by Harris and Jungen [4].

In this Letter we report experimental results and a preliminary analysis of core-penetrating Rydberg states of the BaF molecule. A *complete manifold* of ten core-penetrating Rydberg series (four $^2\Sigma^+$, three $^2\Pi$, two $^2\Delta$, and one $^2\Phi$) with orbital angular momentum $l \leq 3$ is characterized over a range of effective principal quantum number $4.4 < n^*_{l\lambda} < 14.3$. These ten core-penetrating Rydberg series comprise *all* of the components of a series of severely l-mixed $s \sim p \sim d \sim f$ supercomplexes. The present spectra represent one of the most comprehensive experimental examples of a series of molecular Rydberg supercomplexes as well as the first example of a $s \sim p \sim d \sim f$ supercomplex. A significantly more accurate value of the adiabatic ionization potential of BaF, $38\,742 \pm 3$ cm^{-1}, was derived from the experimental data.

The present experiments on highly polar diatomic molecules address uniquely molecular (as opposed to atomic) mechanisms of energy and angular momentum exchange between the Rydberg electron and the ion core. The simplest mechanism is long-range (i.e., outside the core) e^-/MX^+ electrostatic interaction owing to the core electric dipole, quadrupole, and higher multipole moments and multipole polarizabilities. The extra-core long-range mechanisms can cause l mixing among core-penetrating states as well as between core-penetrating and -nonpenetrating states [5]. Intracore processes involve more complex energy exchange mechanisms. These intracore dynamics are encoded exclusively in the core-penetrating series, primarily in the form of severe l mixing among the low-l series. A key simplifying factor is, however, that only a limited number of l values are mixed by intracore processes. This Letter will focus on the core-penetrating $s \sim p \sim d \sim f$ supercomplex series of BaF.

Apart from an $(n^*_{l\lambda})^{-3/2}$ amplitude scale factor, the intracore part of the wave function for each core-penetrating Rydberg state [6] is $n^*_{l\lambda}$ invariant. All information about short-range e^-/ion-core inelastic scattering is encoded in this intracore part of the wave function, which should be well described by an atom-in-molecule model for the valence states, each of which is the low-$n^*_{l\lambda}$ terminus of one core-penetrating Rydberg series. The alkaline earth monohalide valence states can be well described by a zero-order model comprised of two closed shell atomic ions in the core (M^{2+} and X^-) and a single nonbonding electron [7].

The present study of the BaF molecule was undertaken to explore more completely several effects first observed in the spectrum of the CaF molecule [1-4]. The electronic structure of BaF is more complex than that of CaF, but it can still be simply related to the spectrum of the Ba$^+$ ion. When spherical symmetry is broken in the BaF molecule and the Λ (projection of the orbital angular momentum onto the internuclear axis) degeneracy is lifted, the four core-penetrating Rydberg series (s, p, d, and f) of the Ba$^+$ ion [8] split into ten molecular Rydberg series, as compared to the six $s \sim p \sim d$ core-penetrating series in CaF. BaF exhibits a much stronger spin-orbit interaction than CaF, which is fortunate because the spin-orbit interaction is an excellent diagnostic of intracore l-mixing processes [3], especially in $\Lambda > 1$ states (two $^2\Delta$ and one $^2\Phi$ series in the BaF molecule as compared to only one $^2\Delta$ series in CaF). In $\Lambda > 1$ states the Rydberg electron is centrifugally excluded from the region of the internuclear axis, thus the core-penetration effects encoded in these states are expected to be due primarily to penetration of the Rydberg electron into the M^{2+} ion. In addition, BaF is a rare example of a diatomic molecule where the ionization potential (38 742

0031-9007/94/72(14)/2167(4)$06.00

cm^{-1}) is smaller than the dissociation energy [9], $D_0^0 = 48\,800$ cm^{-1}. As a result the rovibronic structures of all BaF (single-electron-excited) Rydberg series converging to the BaF$^+$ $X^1\Sigma^+$ molecular ion are profoundly simplified because these series are free of perturbations by repulsive or weakly bound $^2\Pi$ or $^2\Sigma^+$ covalent states which dissociate adiabatically to $M(^1S)+X(^2P)$ neutral atoms.

Our experimental setup is similar to that described by Murphy *et al.* [1]. BaF molecules are produced in a high-temperature ($T \sim 1200$ K) oven by resistive heating of BaF$_2$ crystals and a small amount of boron in a graphite crucible. Flowing argon, at a pressure of about 200 mTorr, is used as a carrier gas. A pulsed optical-optical double resonance (OODR) fluorescence excitation scheme probes the BaF Rydberg states. The pump laser (Spectra Physics, PDL-1) selectively populates individual rotational levels of the intermediate vibronic state ($C^2\Pi_{3/2}, v=0$) with levels $6.5 \le J \le 25.5$ for f symmetry and $14.5 \le J \le 25.5$ for e symmetry. Observations via the $J=6.5f$ and $8.5f$ intermediate rovibronic levels are common to the data sets obtained for *all* observed Rydberg states. As the probe laser (Lambda Physik, FL3002E) is scanned, the OODR spectrum (see Fig. 1) is recorded by detecting direct or cascade UV fluorescence from Rydberg states down to the $X^2\Sigma^+$ ground state. Both dye lasers are pumped by the same Nd:YAG laser (Quanta Ray, DCR-2A) and operated with intracavity etalons. Extreme congestion of the pump transition spectrum ($C^2\Pi_{3/2}$-$X^2\Sigma^+$), caused by the similarity of rotational and vibrational molecular constants in the $X^2\Sigma^+$ and $C^2\Pi_{3/2}$ states, prevents us from accessing rotational levels with $J < 6.5$ for f symmetry and $J < 14.5$ for e symmetry.

74 new electronic states are observed and characterized. Although we focus on $v=0$ vibrational levels in the present project, levels with $v=1$, 2, and 3 are also detected (a total of 130 vibronic levels). $v=0$ levels are easily identified because the $(v',v'')=(0,0)$ pump transition is isotopically unselective and probe transitions terminating on $v>0$ Rydberg states exhibit diagnostically useful resolved Ba isotope splittings. For *each* of the 130 Rydberg vibronic states, between 5 and 30 scans are recorded by pumping different, systematically selected, intermediate J levels. Altogether more than 2000 spectral lines are recorded, measured, and assigned. The $^2\Sigma^+$ and $^2\Delta$ Rydberg states ($\Delta\Lambda = \pm 1$ probe transitions) usually require fewer scans because, out of the f symmetry levels in the intermediate state, *both* f (P and R branches) and e (Q branch) symmetry levels are accessed in the Rydberg states. For $^2\Pi$ Rydberg states ($\Delta\Lambda = 0$ probe transitions) it is necessary to record many more scans (up to 30) for each vibronic state because the Q branches are weak and usually unobservable. To access e symmetry levels in $^2\Pi$ states it is necessary to pump e levels in the intermediate $C^2\Pi_{3/2}$ state. Since the lowest accessible overlap-free e symmetry J level in the intermediate state is $J=14.5$, it became necessary to obtain spectra for consecutive J values up to at least $J=20.5$ for both e and f symmetry in order to assign spectra conclusively. In addition, the assignment and fitting of the spectra are further complicated by multiple but systematic perturbations by members of $l>3$ series. These perturbations, and the nonpenetrating series they reveal, will be discussed in a future publication.

The Rydberg states' electronic term values ($T_{n^*\lambda}$) can be described by the well known Rydberg formula

$$T_{n^*l\lambda} = \mathrm{IP} - R_{\mathrm{BaF}}/(n^*_{l\lambda})^2, \tag{1}$$

where $n^*_{l\lambda} = n - \mu_{l\lambda}$ is the effective principal quantum number, $\mu_{l\lambda}$ is the quantum defect, n is the principal quantum number (integer), IP is the adiabatic ionization potential, and R_{BaF} is the Rydberg constant (109 737 cm^{-1}). The ionization potential is an adjustable parameter in Eq. (1). It was varied to satisfy the requirement that the quantum defect $\mu_{l\lambda}$ be asymptotically constant for each Rydberg series. The value of the ionization potential, IP$=38\,742 \pm 3$ cm^{-1}, obtained this way is in

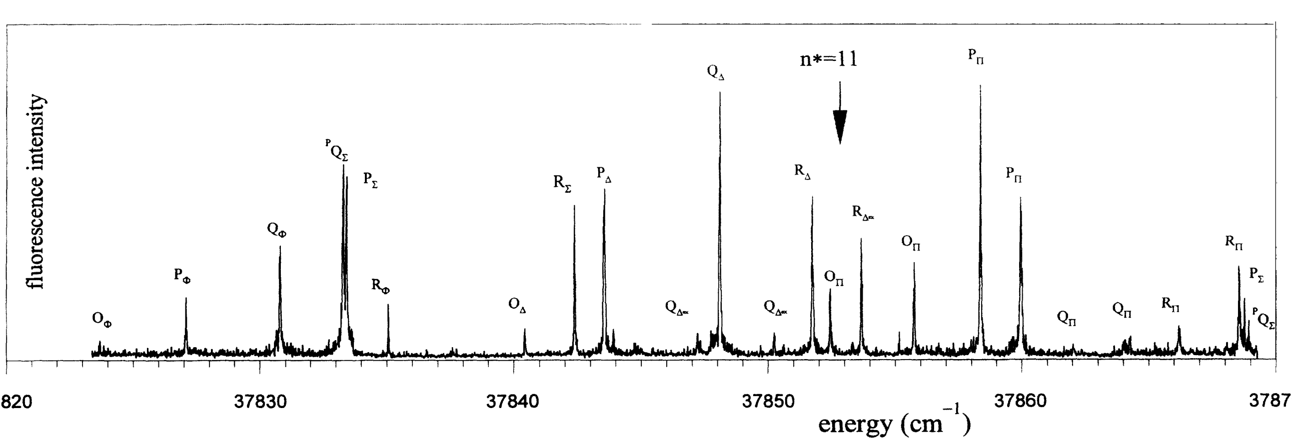

FIG. 1. A spectrum of the $n^* \approx 11$ region, originating from the $C^2\Pi_{3/2}$, $v=0$, $J=8.5f$ intermediate level. It is one of the 18 spectra from which the reduced term value plot in Fig. 3 is constructed.

good agreement with IP = 37900 ± 800 cm^{-1} (recently measured in an electron-impact experiment [10]), but much more precise. All of the newly observed electronic states, together with all previously known states (denoted by their letter name), are presented in Fig. 2 in the form of a plot of $n_{l\lambda}^*$ mod1 vs $n_{l\lambda}^*$. States belonging to the same Rydberg series are connected by tie lines. Membership in each series is based on the similarity of quantum defects and the proper scaling behavior [3] of the fine structure molecular constants. All but two of the ten core-penetrating Rydberg series could be followed up to $n_{l\lambda}^* \approx 14$. Two of the series, 0.46 $^2\Pi$ and 0.76 $^2\Sigma^+$, could not be observed in our OODR spectra above $n_{l\lambda}^* = 7$. The convention for naming Rydberg series, for example, 0.46 $^2\Pi$, specifies the series of $^2\Pi$ states with $n_{l\lambda}^*$ mod1 equal to ~ 0.46. Observation of the $^2\Phi$ series was unexpected because the intermediate state was a $^2\Pi$ state and $\Delta\Lambda = 2$ transitions are forbidden. However, due to l uncoupling effects (Λ mixing among the Rydberg states), spectra of the $^2\Phi$ state were first detectable at $n_{l\lambda}^* = 8.86$ and, up to the highest observed $n_{l\lambda}^* = 13.86$ member, the intensity of the transitions into the nominal $^2\Phi$ states increased monotonically.

As one can see in Fig. 2, for $n_{l\lambda}^* > 4.5$ (the Rydberg region) the quantum defects are approximately constant within each series. Also, fine structure constants follow the scaling relationships described in Ref. [3]. We observe, consistent with the scaling rules, the spin-rotation parameters, γ, to be nearly independent of $n_{l\lambda}^*$ within each series and having the following preliminary values -0.02, 0.01, -0.2, and 0.04 cm^{-1} for the 0.88, 0.77, 0.24, and 0.08 $^2\Sigma^+$ series, respectively. A few states exhibit deviations of their spin-rotation parameter from the nominal value for the series. All of the deviations can be explained as due to perturbations by known $v > 0$ states. The spin-orbit parameters for both the 0.94 and 0.24 $^2\Delta$ series obey the $(n_{l\lambda}^*)^{-3}$ scaling law. The scaled values, $A(n_{l\lambda}^*)^3$, are respectively 13 and 930 cm^{-1}. The latter value (for 0.24 $^2\Delta$ series) agrees satisfactorily with our ligand field model result (900–1000 cm^{-1}; 55%d-45%f l character) [11,12]. However, our calculated scaled spin-orbit constant for the 0.94 $^2\Delta$ series is almost a factor of 20 larger than the experimental one. Such a disagreement remains unexplained so far. The spin-orbit scaling should also apply to the $^2\Pi$ states. However, the three $^2\Pi$ series remain incompletely analyzed and their molecular constants are not yet available. The molecular fine structure constants (A,p,q,γ), accurate values of which will eventually be derived from the core-penetrating spectra, will provide a direct view of the e^-/MX^+ intracore interaction [3]. Such a fine structure based view is complementary to the information conveyed by the electronic energy levels (or quantum defects) [2,4].

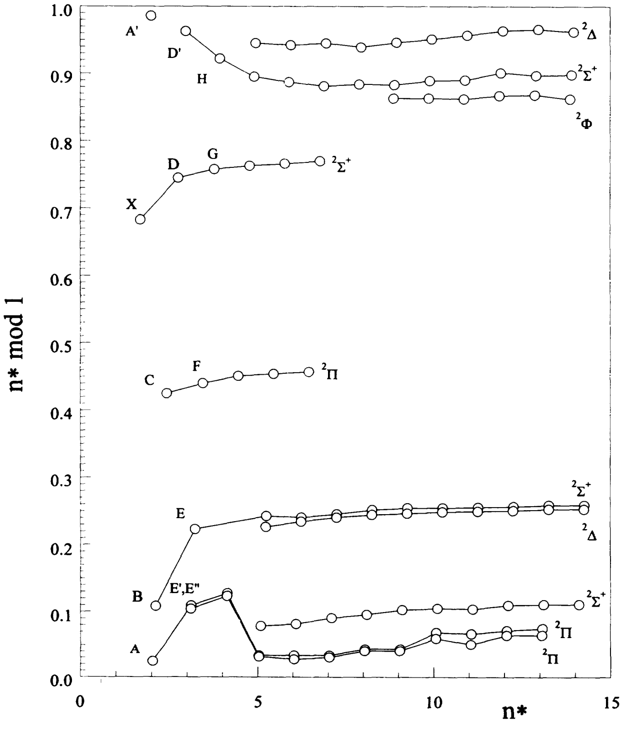

FIG. 2. $n_{l\lambda}^*$ mod1 vs $n_{l\lambda}^*$ plot for all known electronic Rydberg states of BaF. The states known prior to this project are denoted by their letter names.

In the pre-Rydberg $n_{l\lambda}^* < 4.5$ region (see Fig. 2) most of the series depart significantly from constant quantum defect behavior. Those variations of the quantum defect can be explained by two effects. First, the wave functions for the low-$n_{l\lambda}^*$ core-penetrating states are localized much closer to the Ba^{2+} ion than their $n_{l\lambda}^* > 4.5$ Rydberg counterparts ($Z_{\text{eff}} \approx 1$), thus they experience additional attraction ($Z_{\text{eff}} > 1$) which lowers their energy (and $n_{l\lambda}^*$) and increases their quantum defects. Similar behavior of the low-$n_{l\lambda}^*$ core-penetrating states of CaF was observed and discussed [1–3]. Second, in the region of $n_{l\lambda}^*$ between 3 and 5, the quantum defects of some of the states decrease abruptly by ~ 0.1–0.2. This second effect is evident (see Fig. 2) even though some of the states in this low-$n_{l\lambda}^*$ region remain unobserved. This type of discontinuity in quantum defect is likely related to the irregular behavior of the f series in the spectrum of the Ba^+ atomic ion. The first members of the Ba^+ f series have anomalously small quantum defects. The quantum defect of the $4f$ state is smaller by as much as 0.55 than the asymptotic value of the series (0.86) [8]. This anomaly is explained by the double well potential experienced by the f electrons in the Ba^+ ion [13]. The quantum defect deviations in the BaF *molecular* Rydberg series are significantly smaller than the corresponding deviations in the f Rydberg series of Ba^+. We attribute this to the dilution of the $4f$ atomic character into many molecular states.

In Fig. 3 we present a reduced term value plot for the $v = 0$ states in the vicinity of $n_{l\lambda}^* = 11$. Four of these states, 11.10 $^2\Sigma^+$, one of the near-degenerate pair of 11.05 $^2\Pi$ states, the 10.96 $^2\Delta$, and the 10.86 $^2\Phi$, are for-

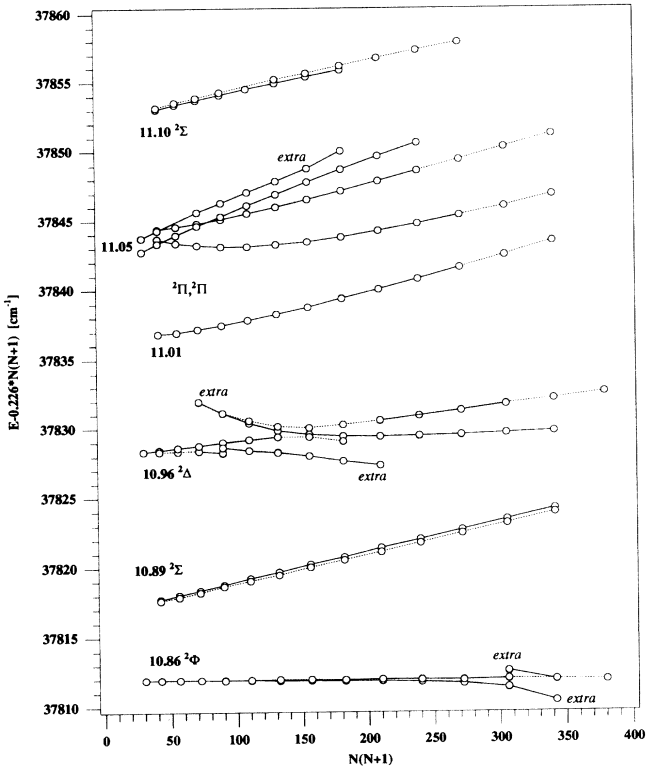

FIG. 3. Reduced term value plot of the $v=0$ states in the vicinity of $n^*_{l\lambda}=11$. [Solid (dotted) line for f (e) symmetry levels.] The extra term at $n^*_{l\lambda}=11.05$ as well as terms perturbing the 10.96 $^2\Delta$ and 10.86 $^2\Phi$ states probably belong to the 11g or 11h complexes.

mally assigned as the four components of an f complex. From the $^2\Delta \leftrightarrow {}^2\Phi$ splitting (~ 16 cm^{-1}), assumed to be due exclusively to the long-range interaction of the Rydberg electron with the core, the BaF$^+$ ion-core quadrupole moment is estimated to be 11 ± 1 a.u. This agrees acceptably with the 12.4 a.u. calculated using a two-point-charge model (+2 charge on the Ba^{2+} and -1 charge on the F$^-$, origin at center of mass). In Fig. 3 multiple perturbations, especially in the 0.96 $^2\Delta$ and 0.86 $^2\Phi$ states, are evident. Similar perturbations were detected for all $n^*_{l\lambda} \geq 7.8$ members of those series. Since all ten core-penetrating series of the $s \sim p \sim d \sim f$ supercomplex are already fully accounted for, we conclude that the perturbing states must be members of $l > 3$ nonpenetrating complexes. The perturbations are due to BaF$^+$ dipole and quadrupole induced interactions between core-penetrating nominally f states and core-nonpenetrating g and h complexes. Our analysis and interpretation of the nonpenetrating states will be published separately.

We are currently working on a global $s \sim p \sim d \sim f$ supercomplex fit of the experimental data described here. Our experimental work is concentrated on the perturbations in the near integer-$n^*_{l\lambda}$ regions (where all of the nonpenetrating states originate), with the goal of extracting sufficient information to characterize the g and h complexes. This would yield much more precise estimates of the BaF ionization potential and values of the BaF$^+$ ion-core electric multipole moments and polarizabilities.

The results are presented of our initial analysis of an extensive set of very precise observations (more than 2000 spectral lines, experimental precision of ~ 0.01 cm^{-1}) of the core-penetrating series of BaF for the $6.5 \leq J \leq 25.5$ range of rotational levels. *All* ten core-penetrating Rydberg series are observed and characterized. Despite its constituent atoms undistinguished locations in the periodic table, the BaF molecule is providing fundamental insights into the mechanisms for exchange of energy and angular momentum between an electron and a molecular cation. The e^-/MX^+ inelastic scattering mechanisms encoded in the Rydberg spectra of BaF are universal; they will be present (if not dominant) and must be taken into account in all heteroatomic molecules. The diagnostics, scaling relationships, and analysis schemes being developed for the spectra of the alkaline earth monohalides illustrate new "beyond molecular constants" strategies for acquiring and organizing both high resolution spectroscopic data and state-of-the-art *ab initio* electronic structure calculations.

The authors are indebted to Dr. James E. Murphy for numerous helpful conversations and to Dr. John M. Berg and Nicole A. Harris for their advice in the initial stages of our experiment. We also thank Dr. Ch. Jungen and Dr. J. K. G. Watson for their interest and helpful discussions. This research is supported by the National Science Foundation under Grant No. CHE91-20339. One of us (Z.J.J.) is also indebted to the Fulbright Program for a Fulbright Fellowship.

[1] J. E. Murphy, J. M. Berg, A. J. Merer, N. A. Harris, and R. W. Field, Phys. Rev. Lett. **65**, 1861 (1990).

[2] J. E. Murphy, Ph.D. thesis, Dept. of Chemistry, Massachusetts Institute of Technology, 1992 (unpublished).

[3] J. M. Berg, J. E. Murphy, N. A. Harris, and R. W. Field, Phys. Rev. A **48**, 3012 (1993).

[4] N. Harris and Ch. Jungen, Phys. Rev. Lett. **70**, 2549 (1993).

[5] J. K. G. Watson (to be published).

[6] R. S. Mulliken, J. Am. Chem. Soc. **86**, 3183 (1964).

[7] S. F. Rice, H. Martin, and R. W. Field, J. Chem. Phys. **82**, 5023 (1985).

[8] C. E. Moore, *Atomic Energy Levels*, NBS, National Standards Reference Data Series Circular No. 35 (U.S. GPO, Washington, DC, 1971).

[9] D. L. Hildenbrand, J. Chem. Phys. **48**, 3657 (1968).

[10] Z. J. Jakubek, N. A. Harris, R. W. Field, J. A. Gardner, and E. Murad, J. Chem. Phys. **100**, 622 (1994).

[11] Z. J. Jakubek and R. W. Field (unpublished).

[12] Z. J. Jakubek and R. W. Field, J. Chem. Phys. **98**, 6574 (1993).

[13] J. P. Connerade, Contemp. Phys. **19**, 415 (1978), and references therein.